THE JOURNAL OF PHYSICAL CHEMISTRY B

ARTICLE

pubs.acs.org/JPCB

On the Interpretation of Quantum Coherent Beats Observed in Two-Dimensional Electronic Spectra of Photosynthetic Light Harvesting Complexes

Akihito Ishizaki and Graham R. Fleming*

Department of Chemistry, University of California, Berkeley, California 94720, United States

Physical Biosciences Division, Lawrence Berkeley National Laboratory, Berkeley, California 94720, United States

ABSTRACT: The observation of long-lived electronic quantum coherence in a photosynthetic light harvesting system [Engel et al. *Nature* **2007**, *446*, 782] has led to much effort being devoted to elucidation of the quantum mechanisms of the photosynthetic excitation energy transfer. In this paper we examine the question of whether the decay of the coherent beating signal is due to quantum mechanical decoherence or ensemble dephasing (also called "fake decoherence"). We compare results based on the quantum master equation description of the time-evolution of the reduced density matrix with a mixed quantum/classical approach where the ensemble average is calculated after the dynamics. The two methods show good agreement with results from the quantum master equation in terms of the decay of quantum coherent oscillations when ensemble average is considered for the mixed quantum/classical approach. However, the results also demonstrate it remains possible that the quantum coherent motion is robust under individual realizations of the environment-induced fluctuations contrary to intuition obtained from the reduced density matrices, indicating that the decay of the observed quantum coherence should be understood as ensemble dephasing. Our calculations imply that coherence is a property of the pigment−protein system, not simply the preparation method of the electronic excitation.

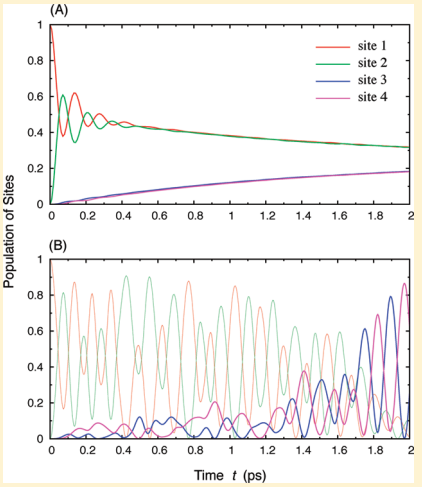

INTRODUCTION

Great strides in femtosecond laser technology have opened up real-time observation of dynamical processes in complex chemical and biological systems. Recently, techniques of two-dimensional electronic spectroscopy[1] have been applied to explore photosynthetic light harvesting complexes and revealed the existence of long-lived quantum coherence among the electronic excited states of the multiple pigments in pigment−protein complexes (PPCs).[2] Although the coherence in the PPCs was originally observed outside the physiological range of temperatures,[2−4] recent experiments detected the presence of quantum coherence lasting up to ∼300 fs even at physiological temperatures,[5,6] which is consistent with a previous theoretical prediction.[7] These observations have led to the suggestion that quantum coherence might be vital in achieving the remarkable efficiency of photosynthetic light harvesting. As we will describe in more detail below, the purpose of this paper is to understand more fully the origin of the experimentally observed decay of quantum coherence.

One of the viable approaches to explore photosynthetic excitation energy transfer (EET) is a quantum master equation.[8] In this approach, one focuses attention only on the electronic excitation, which is termed the system, and treats the other degrees of freedom (DOFs) as the environment. The key quantity of interest is the reduced density matrix (RDM), i.e., the partial average of the total density matrix $\rho_{\mathrm{tot}}(t)$ over the environmental DOFs: $\rho(t) = \mathrm{Tr}_{\mathrm{env}}[\rho_{\mathrm{tot}}(t)]$. This matrix can be naturally introduced via the expectation value of a system's operator $\mathcal{O}_{\mathrm{sys}}$ as $\mathrm{Tr}_{\mathrm{tot}}[\mathcal{O}_{\mathrm{sys}}\rho_{\mathrm{tot}}(t)] = \mathrm{Tr}_{\mathrm{sys}}[\mathcal{O}_{\mathrm{sys}}\rho(t)]$. In the literature of photosynthetic EET, the initial condition of the environmental DOFs is assumed to be the thermal equilibrium state $\rho_{\mathrm{env}}^{\mathrm{eq}}$, which is a mixed state, because of the lack of information on the environmental DOFs. Thus, the total density matrix is expressed as

$$\rho_{\mathrm{tot}}(t) = \mathrm{e}^{-iH_{\mathrm{tot}}t/\hbar}[\rho_{\mathrm{sys}}(0) \otimes \rho_{\mathrm{env}}^{\mathrm{eq}}]\mathrm{e}^{iH_{\mathrm{tot}}t/\hbar} \quad (1)$$

with H_{tot} being the total Hamiltonian. This mixed-state density matrix formalism is often employed to describe a true physical ensemble, i.e., a collection of multiple identical physical systems. Consequently, approaches of this type have a considerable domain of applicability, for instance in analyses of condensed phase spectroscopic signals.[9] Experimentally, photosynthetic EET dynamics are investigated by synchronizing initial electronic excitation in the entire ensemble by means of ultrashort laser pulses. In natural light harvesting, however, the initial event is the absorption of one sunlight photon by a single PPC, followed by

Received: December 31, 2010
Revised: February 25, 2011
Published: April 13, 2011

EET in the PPC independently of the ensemble averaged behavior or our measurements.

It is undeniable that the RDM approach based on eq 1 has provided useful insight into condensed phase spectra and photosynthetic EET.[8,9] However, considering the difference between electronic excitation dynamics in individual PPCs and their ensemble average naturally raises the question as whether such an approach might limit understanding of the EET because the reduction procedure involves an ensemble average which may wash out the microscopic details. In particular, this issue becomes prominent when quantum coherence and its destruction are discussed. In the literature, descriptions of several different processes are sometimes referred to as "decoherence."[10,11] Most of these associations are based on the observation that different processes may all lead to the disappearance of off-diagonal elements in the density matrix of the system. Reference 11 describes decoherence and "fake decoherence". According to ref 11 decoherence should be understood as a distinctly quantum mechanical effect with no classical analog, independently of an ensemble average. When both the system and its environment are described quantum mechanically, the interaction between them leads to a quantum entangled state for the system−environment combination, $|\psi^{\mathrm{tot}}(t)\rangle = \Sigma_n c_n(t)|\varphi_n^{\mathrm{sys}}\rangle|\theta_n^{\mathrm{env}}(t)\rangle$, where $|\varphi_n^{\mathrm{sys}}\rangle$ is a system's state in some basis and $|\theta_n^{\mathrm{env}}(t)\rangle$ describes time-evolution of the environmental state associated with $|\varphi_n^{\mathrm{sys}}\rangle$. This entanglement implies that the system and its environment share information on the system. However, measurements are usually performed only on the system, whereas the environment is typically either inaccessible or simply of no interest. Thus, the shared information is also inaccessible, and it means that a portion of the information on the system is lost as long as observers only are able to measure observables that pertain to the system. This process corresponds to decoherence. Tracing over the inaccessible environmental states yields an RDM of the entangled subsystem as

$$\rho_{\mathrm{red}}(t) = \sum_{mn} c_m(t)c_n^*(t)|\varphi_m^{\mathrm{sys}}\rangle\langle\varphi_n^{\mathrm{sys}}|\langle\theta_m^{\mathrm{env}}(t)|\theta_n^{\mathrm{env}}(t)\rangle \qquad (2)$$

After a sufficiently long time, an environmental state $|\theta_m^{\mathrm{env}}(t)\rangle$ diverges maximally, and thus overlaps between the environmental states associated with the different $|\varphi_m^{\mathrm{sys}}\rangle$ become small. Thus, the $\{|\theta_n^{\mathrm{env}}(t)\rangle\}$ become mutually orthogonal, $\langle\theta_m^{\mathrm{env}}(t)|\theta_n^{\mathrm{env}}(t)\rangle \overset{t\to\infty}{\longrightarrow} \delta_{mn}$, resulting in the disappearance of the off-diagonal elements in eq 2. Following these lines of thought, the appearance of a classical world in quantum theory has been explored.[11−14] On the other hand, an example of "fake decoherence"[11,14] is to interpret the result of an ensemble average over different noisy realizations of a system as the description of a decoherence process. As was mentioned above, the density matrix formalism is often used to describe a true physical ensemble, i.e., a collection of multiple physical systems in which each individual system is described by a pure state, $|\psi^{(n)}(t)\rangle$.[11] In this situation, each system may start out in the same state but may be subject to slightly different Hamiltonians. For example, the Hamiltonian of each system may contain random fluctuations due to the presence of classical noise. If we take the average over the ensemble $\{\psi^{(n)}(t)\}$ of the pure states of all N systems, the ensemble density matrix is obtained as

$$\rho_{\mathrm{ensemble}}(t) = \frac{1}{N}\sum_{n=1}^{N} |\psi^{(n)}(t)\rangle\langle\psi^{(n)}(t)| \qquad (3)$$

In the limit of large N, the off-diagonal elements of the ensemble density matrix would disappear. This is evidently ensemble dephasing, not decoherence.

We can now sharpen the statement made above on the purpose of the paper. In principle, both the electronic excitations and the rest of the entire universe should be described quantum mechanically, as described in eq 2. In practice, however, the protein environments embedding pigments are usually assumed to be classical objects and to induce classical noise in the electronic energies of the pigments. The statement that biological systems are "warm, wet, and noisy environments" is essentially a classical aspect of proteins, membranes, and so on. Furthermore, the protein environment are also surrounded by their environments, and thus they would be decohered in the sense of eq 2. Clearly this discussion can be continued *ad infinitum*. A decision on whether the protein environments should be treated quantum mechanically is intimately related to the specific experimental observable and appears to us to have no universal answer. Therefore, it is not obvious to what extent quantum features of the protein environment play a role in decoherence of electronic excitations. Consequently, it is not obvious whether the decay of quantum coherent beats observed in two-dimensional electronic spectra of photosynthetic PPCs is describing decoherence or ensemble dephasing. In this paper we try to answer this question by means of mixed quantum/classical simulations.[15−18] In addition, despite the very good agreement between the ensemble experiments and the ensemble averaged theory, it is still tempting to ask questions such as (1) How does EET proceed in a single PPC? (2) Does the initial coherence just decay irreversibly or can it recur? (3) Can coherence appear in a PPC excited not by light, but by EET from another PPC? (4) How relevant are the laser-based results to photosynthesis in natural sunlight? Answers to these questions have been discussed or assumed in numerous recent publications.[19−38] However, providing a precise answer to these questions requires an approach that looks at the dynamics prior to the ensemble average with respect to the mixed state or more specifically the thermal distribution for environmental DOFs. In this paper we begin the exploration of such an approach by employing a mixed quantum/classical simulation under the assumption that the protein environments induce classical noise in electronic energies of the embedded pigments. In our approach, only the electronic excitation is treated quantum mechanically, while the environmental DOFs are described as classical variables. The combination of two fundamentally different descriptions of nature provided by quantum and classical mechanics might cause serious problems of consistency. In order for such contradictions to be minimized to an acceptable level, we assume that the quantum mechanical action of the system on the environment can be ignored. Thus, it is of no consequence that completely classical environmental DOFs violate the uncertainty principle. The Hamiltonian for a pure quantum state is time-dependent because it contains random fluctuations due to the presence of classical noise. This assumption corresponds to stochastic approaches such as the temperature-independent Lindblad equation or the Haken-Strobl model,[39] which are extensively employed for examining quantum effects in photosynthetic EET.[30−37,40,41] For this reason we think this assumption is of minor consequence for the present purpose.

MODEL

In this paper, the electronic spectrum of the mth pigment is restricted to the ground state $|\varphi_{mg}\rangle$ and the first excited

state $|\varphi_{me}\rangle$ which corresponds to the Q_y transition in a (bacterio)chlorophyll molecule. These states are obtained by the electronic Schrödinger equation $H_m^{el}(X)|\varphi_{ma}\rangle = \varepsilon_{ma}(X)|\varphi_{ma}\rangle$, where $H_m^{el}(X)$ and $\varepsilon_{ma}(X)$ are the electronic Hamiltonian and energy of the mth pigment in the absence of the interpigment electronic coupling, and depend parametrically on the set of the relevant nuclear coordinates including protein environmental DOFs, X. Hence, the nuclear dynamics associated with an electronic state $|\varphi_{ma}\rangle$ are described by $H_{ma}(X) \equiv \varepsilon_{ma}(X) +$ (kinetic energy). The normal mode treatment is usually assumed for the PPC nuclear dynamics, because anharmonic motion with large amplitudes and long time scales produces inhomogeneous broadening on time scales irrelevant to photosynthetic EET.[9,42,43] Further, it may be assumed that nuclear configurations for the electronic excited states of pigments are not greatly different from those for the ground states owing to the absence of large permanent dipoles on the pigments. Thus, the nuclear Hamiltonians associated with the electronic states $|\varphi_{mg}\rangle$ and $|\varphi_{me}\rangle$ can be modeled as a set of displaced harmonic oscillators:

$$H_{mg}(X) = \varepsilon_{mg}(X_{mg}^0) + \sum_\xi \frac{\hbar\omega_{m\xi}}{2}(p_{m\xi}^2 + q_{m\xi}^2) \tag{4}$$

$$H_{me}(X) = H_{mg}(X) + \hbar\Omega_m - \sum_\xi \hbar\omega_{m\xi} d_{m\xi} q_{m\xi} \tag{5}$$

where $\{q_{m\xi}\}$ are the dimensionless normal mode coordinates introduced around the equilibrium nuclear configuration associated with the mth pigment X_{mg}^0, and $\{\omega_{m\xi}\}$ and $\{p_{m\xi}\}$ are the accompanying frequencies and momenta. The energy $\hbar\Omega_m$ is the Franck−Condon transition energy of the mth pigment, which is termed the site energy in the literature. The dimensionless quantity $d_{m\xi}$ denotes the displacement of the equilibrium configuration of the ξth environmental mode between the ground and excited electronic states of the mth pigment. In what follows, we set $\varepsilon_{mg}(X_{mg}^0) = 0$ to simplify our expressions.

For characterizing the possible states of the whole complex of excitable units, product states are introduced as $\Pi_m|\varphi_{ma_m}\rangle$. The overall ground state with zero excitation reads $|0\rangle \equiv \Pi_m|\varphi_{mg}\rangle$, whereas the presence of a single excitation at the mth pigment is described by $|m\rangle \equiv |\varphi_{me}\rangle\Pi_{k(\neq m)}|\varphi_{kg}\rangle$. Since the intensity of sunlight is weak, the single-excitation manifold comprising one elementary excitation is of primary importance under physiological conditions. Thus, only the single-excitation manifold is considered, and the PPC Hamiltonian is given as

$$H_{PPC}^{(1)} = \sum_m H_m(X)|m\rangle\langle m| + \sum_{mn} \hbar J_{mn}|m\rangle\langle n| \tag{6}$$

with $H_m(X)$ being defined as

$$H_m(X) = H_{me}(X) + \sum_{k(\neq m)} H_{kg}(X) \tag{7}$$

We note the completeness relation in the single-excitation manifold, $\Sigma_m|m\rangle\langle m| = 1$. Although the electronic coupling $\hbar J_{mn}$ may be also modulated by nuclear motions,[44] we assume that nuclear dependence of $\hbar J_{mn}$ is vanishingly small and employ the Condon-like approximation as usual.

From the dynamical point of view, eqs 4, 5, and 6 demonstrate that the electronic energies of the pigments experience modulation by the protein motion. Due to the large number of protein DOFs, such dynamical modulation can be modeled as random fluctuations. In order to describe fluctuations in electronic states, the collective energy gap coordinate is introduced as[9]

$$u_m \equiv H_{me}(X) - H_{mg}(X) - \hbar\Omega_m \tag{8}$$

Because $\{q_{m\xi}\}$ in eqs 4 and 5 are normal mode coordinates or phonon modes, the dynamics of $u_m(t) \equiv e^{iH_{mg}t/\hbar} u_m e^{-iH_{mg}t/\hbar}$ can be described as a Gaussian process.[45] Therefore, the environmental effects can be characterized fully by two-point correlation functions of $u_m(t)$, e.g., the symmetrized correlation function:

$$S_m(t) = \frac{1}{2}\langle\{u_m(t), u_m(0)\}\rangle_{mg} = \frac{\hbar}{\pi}\int_0^\infty d\omega \mathcal{J}_m(\omega) \coth\frac{\beta\hbar\omega}{2}\cos\omega t \tag{9}$$

where $\langle\ldots\rangle_{mg}$ denotes averaging over $\rho_{mg}^{eq} = e^{-\beta H_{mg}}/\mathrm{Tr}[e^{-\beta H_{mg}}]$ with β being the inverse temperature. The spectral density $\mathcal{J}_m(\omega)$ is given in terms of the displacement $d_{m\xi}$ as $\mathcal{J}_m(\omega) = (\pi/2)\Sigma_\xi \hbar\omega_{m\xi}^2 d_{m\xi}^2 \delta(\omega - \omega_{m\xi})$, and the reorganization energy of the mth pigment is expressed as $\hbar\lambda_m = \int_0^\infty d\omega \mathcal{J}_m(\omega)/(\pi\omega) = \Sigma_\xi \hbar\omega_{m\xi} d_{m\xi}^2/2$. In the classical limit ($\hbar \to 0$), eq 9 yields the classical correlation function, $S_m(t) = \langle u_m(t)u_m(0)\rangle_{mg}$. For simplicity, we assume that fluctuations in electronic energies of different pigments are not correlated. Furthermore, we suppose that the environmental state at the initial time $t = 0$ is in thermal equilibrium, ρ_{mg}^{eq}. This initial condition corresponds to an electronic excited state generated in accordance to the vertical Franck−Condon transition.

In this work, we assume the environmental DOFs are described in terms of classical phase space positions and momenta. Under this assumption, electronic excitation dynamics $|\psi(t)\rangle$ is described with the Schrödinger equation involving a time-dependent Hamiltonian:

$$i\hbar\frac{\partial}{\partial t}|\psi(t)\rangle = H_{PPC}^{(1)}|\psi(t)\rangle \tag{10}$$

where the classical path of the environmental DOFs causes fluctuations in electronic energies of pigments, as shown in eqs 4−8. On the other hand, the time-evolution of the environmental DOFs follow the Hamilton equations derived from the Ehrenfest theorem[15] as

$$\dot{p}_{m\xi} = -\omega_{m\xi} q_{m\xi} + f_{m\xi}(t) \tag{11}$$

$$\dot{q}_{m\xi} = \omega_{m\xi} p_{m\xi} \tag{12}$$

where $\hbar f_{m\xi}(t)$ is the Ehrenfest mean-field force given as

$$f_{m\xi}(t) = P_m(t)\omega_{m\xi} d_{m\xi} \tag{13}$$

with $P_m(t) = \langle m|\psi(t)\rangle\langle\psi(t)|m\rangle$ being the probability for excitation to be found on the mth pigment. In the case of $P_m(t) = 0$, the minimum of the harmonic potential for eq 11 and eq 12 is located on $q_{m\xi} = 0$. In the case of $P_m(t) = 1$, on the other hand, the minimum is shifted to $q_{m\xi} = d_{m\xi}$. Thus, the Ehrenfest force causes the reorganization process of the environmental DOFs.[22] However, we do not have a justification of the physical meaning of the force for the case of $0 < P_m(t) < 1$. Indeed, simulations with eqs 10−13 do not produce the appropriate thermal equilibrium of electronic excitation. One of the major accomplishments of the surface-hopping models[46] was to correct this unphysical feature of the mean-field force. In principle, however, the above-mentioned kind of difficulty cannot be removed completely when the mixed quantum-classical approximation is adopted,

because a logical contradiction of physics inevitably arises from the contact of a quantum system with classical DOFs.

In order for such contradiction to be minimized enough to be accepted, we assume the force in eq 11 vanishes,

$$f_{m\xi}(t) \simeq 0 \tag{14}$$

In this approximation, the classical trajectory of the environmental DOFs induce only fluctuations in electronic energies of the pigments; however, the environment does not cause dissipation of reorganization energies. Initial values of $\{p_{m\xi},q_{m\xi}\}$ are chosen with Monte Carlo sampling in accordance with the canonical distribution, $\mathscr{P}_m(\{p_{m\xi},q_{m\xi}\}) \propto e^{-\beta H_{mg}}$. If the number of the environmental modes is large enough, fluctuations in the electronic energies can be regarded Gaussian random modulations. In this manner, temperature and classical stochasticity enter into the dynamics described by eqs 10−14, as in the derivation of the Langevin equation from the Hamilton equation.[47] Although the fluctuation−dissipation relation (FDR) does not hold obviously, eq 14 corresponds to the situation in stochastic theories such as the Kubo−Anderson model[48] and the Haken−Strobl model.[39] The former model is a convenient tool to investigate linebroadening and non-Markovian features of optical signals,[49] while the latter is useful and extensively employed for examining quantum effects in photosynthetic EET.[30−37,40,41] For this reason, we think the approximation in eq 14 is of minor consequence for the purpose of the present work.

DISCUSSION

Numerical results are presented to discuss relations among the RDM, quantum dynamics influenced by individual realizations of fluctuations, and their ensemble average. For simplicity, the Drude−Lorentz spectral density is assumed, $\mathscr{J}_m(\omega) = 2\hbar\lambda_m\tau_m\omega/(\tau_m^2\omega^2 + 1)$, although an arbitrary spectral density can be employed for the present simulations. This density yields the classical correlation function of the collective energy gap coordinate as $S_m(t) = \langle u_m(t)u_m(0)\rangle_{mg} = (2\hbar\lambda_m/\beta)e^{-t/\tau_m}$. For numerical integration of eqs 10−14, the continuum spectral density needs to be discretized. Following ref 50, we introduce a density of frequencies $g_m(\omega)$ and discretize the continuum of frequencies as $\int_0^{\omega_\xi} d\omega\, g_m(\omega) = \xi$ for $\xi = 1, 2, ..., N_m^{\mathrm{mode}}$. The displacement $d_{m\xi}$ for each $\omega_{m\xi}$ is then given by $d_{m\xi}^2 = 2\mathscr{J}_m(\omega_{m\xi})/[\pi\omega_{m\xi}^2 g_m(\omega_{m\xi})]$. The precise functional form of $g_m(\omega)$ does not affect the final answer if enough environmental modes are included. For efficient numerical calculations, however, ref 50 suggested the form of $g_m(\omega) = N_m^{\mathrm{mode}}/(2(\omega\cdot\omega_m^{\mathrm{max}})^{1/2})$, where the discrete frequencies are given as $\omega_{m\xi} = (\xi/N_m^{\mathrm{mode}})^2\omega_{\mathrm{max}}$.

In what follows, the values of $\omega_m^{\mathrm{max}} = 20\tau_m^{-1}$ and $N_m^{\mathrm{mode}} = 1000$ are employed, and the spectral density for the different sites are assumed to be equivalent, i.e., $\lambda_m = \lambda$ and $\tau_m = \tau$. Statistical averages are taken for 50 000 realizations.

Figure 1 shows ensemble averaged behaviors of excitation dynamics in a two-site system calculated from eqs 10−14 for various magnitudes of the reorganization energy λ (solid lines).

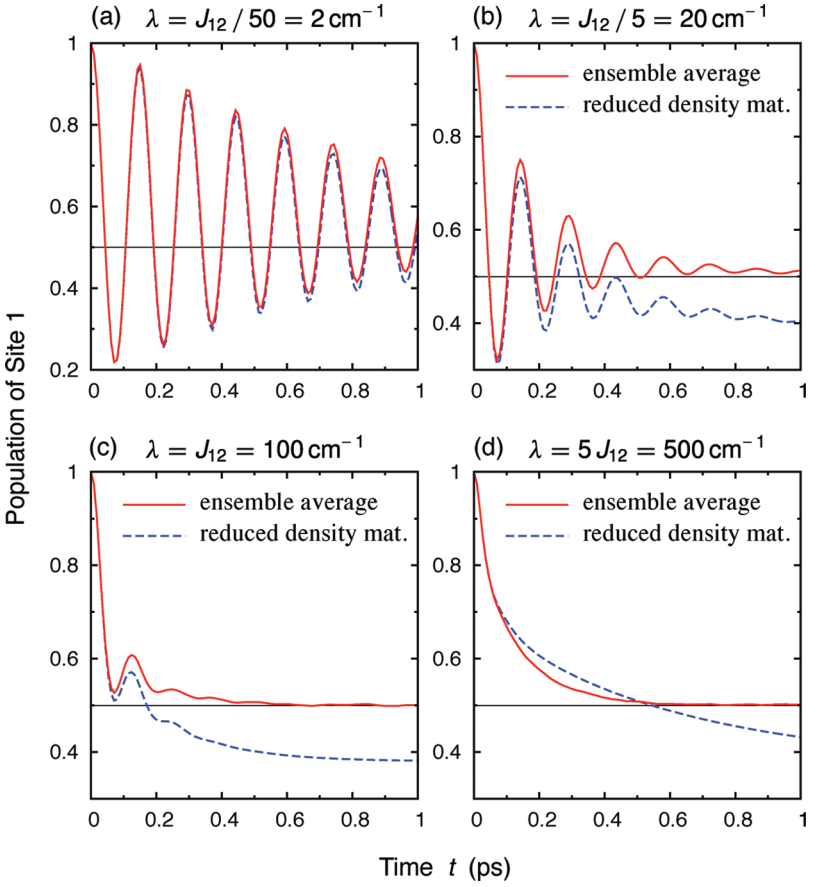

Figure 1. Ensemble averaged time evolution of site 1 population calculated from eqs 10−14 for various magnitudes of reorganization energy λ (solid line). The other parameters are $\Omega_1 - \Omega_2 = 100\ \mathrm{cm}^{-1}$, $J_{12} = 100\ \mathrm{cm}^{-1}$, $\tau = 100$ fs, and $T = 300$ K. For comparison, the dynamics calculated from the RDM are shown (dashed lines; data taken from ref 22).

dx.doi.org/10.1021/jp112406h |J. Phys. Chem. B 2011, 115, 6227–6233

The other parameters are given in the figure caption, which are typical for photosynthetic EET. The dashed lines present dynamics of the RDM calculated for the same parameter set with the second-order cumulant time−nonlocal quantum master equation,[22] which reduces to the conventional Redfield and Förster theories in their respective limits of validity. All the panels in Figure 1 demonstrate that the ensemble average and the RDM show excellent agreement with respect to quantum coherent wave-like behavior and its destruction. However, a clear difference is observed in the longer time region: the RMD results converge to the vicinity of the thermal equilibrium value, whereas the ensemble average converges to 0.5. This difference is explained by the breakdown of the FDR in the present simulation. In the quantum master equation approach, the correlation function $S_m(t)$ satisfies the FDR with the environmental response function $\chi_m(t)$, which describes the reorganization process.[22] In the classical limit, the FDR is expressed as $\chi_m(t) \simeq -\beta(\mathrm{d}/\mathrm{d}t)S_m(t)$, which guarantees that thermal equilibrium is reached at long times. However, we have assumed eq 14, indicating that the reorganization process is vanishing, i.e. $\chi_m(t) = 0$. This situation mathematically corresponds to the infinite temperature limit ($\beta \rightarrow 0$) in the FDR. As a result, the ensemble average converges to "the thermal equilibrium at the infinite temperature." Despite this reasonable artifact, the agreement in terms of the quantum coherent motion implies that the behavior of the RDM can be interpreted as the ensemble average of the quantum dynamics in individual PPCs, i.e., the ensemble dephasing.

Figure 2 presents excitation dynamics in a four-site system calculated from eqs 10−14. The excitation Hamiltonian H_{ex} and the excitation-environment coupling parameters are given in the figure caption. Sites 1−2 and sites 3−4 make two strongly coupled dimers, while the two dimers are weakly coupled. This situation is not unusual in photosynthetic complexes. Figure 2A presents the ensemble averaged behavior corresponding to the RDM. In Figure 2A we observe quantum coherent wave-like motion between sites 1 and 2 up to 500 fs. However, EET in the 3−4 dimer and between the dimers do not exhibit any coherent motion; they are usually regarded as describable as incoherent diffusion. On the other hand, Figure 2B shows time-evolution of the electronic excitations influenced by a particular realization of the environment-induced fluctuations without an ensemble average. Although the ensemble averaged behavior exhibits destruction of the wave-like motion, the individual system excitation dynamics does not. Comparison between panels A and B of Figure 2 clearly demonstrates the quantum coherent effects are washed out in the average or dephasing mechanism. Interestingly, after the "incoherent diffusion" from the 1−2 dimer to the 3−4 dimer, wave-like motion is intensified in the 3−4 dimer contrary to the intuition obtained from the RDM. This implies that existence of electronic quantum coherence does

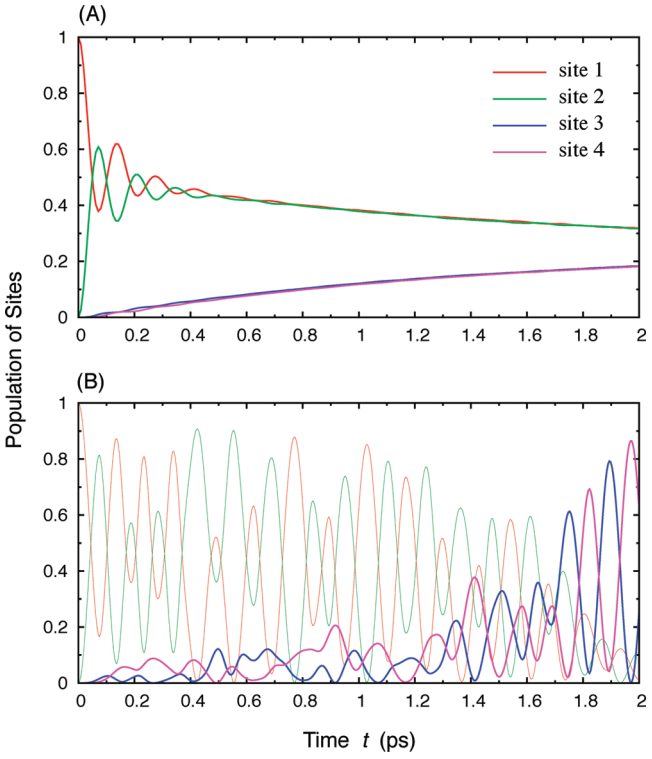

Figure 2. Time evolution of populations in a four-site system. We set $\Omega_1 = \Omega_2 = 200\ \mathrm{cm}^{-1}$, $\Omega_3 = \Omega_4 = 100\ \mathrm{cm}^{-1}$, $J_{12} = J_{34} = 100\ \mathrm{cm}^{-1}$, $J_{23} = 20\ \mathrm{cm}^{-1}$; the other excitonic couplings vanish. The other parameters are $\lambda = 50\ \mathrm{cm}^{-1}$, $\tau = 100$ fs, and $T = 300$ K. The upper panel (A) presents the ensemble averaged behavior, whereas the lower panel (B) shows an individual trajectory of the excitation dynamics without the ensemble average.

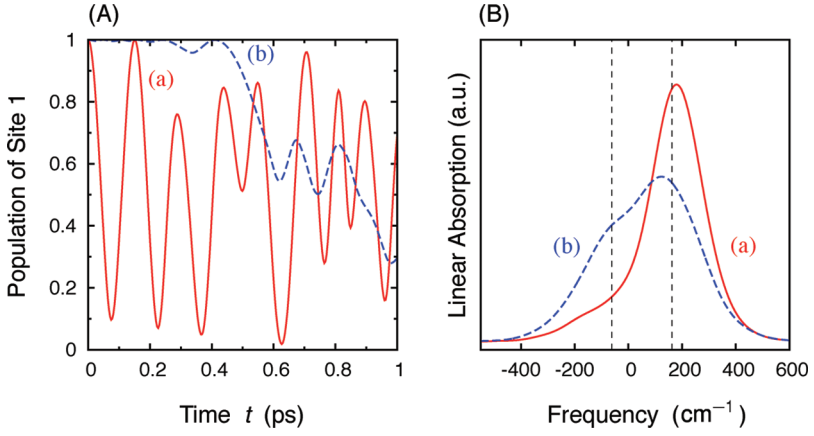

Figure 3. The left panel (A) shows trajectories for excitation dynamics in two-site systems, whereas the right panel (B) gives linear absorption spectra of their ensembles. We consider two cases, (a) $(\Omega_1, \Omega_2, J_{12}) = (100, 0, 100)\ \mathrm{cm}^{-1}$ and (b) $(\Omega_1, \Omega_2, J_{12}) = (160, -60, 20)\ \mathrm{cm}^{-1}$. These introduce the same eigenenergies (161.8, −61.8) cm^{-1} shown by vertical lines in the panel (B). The other parameters are $\lambda = 50\ \mathrm{cm}^{-1}$, $\tau = 100$ fs, and $T = 300$ K. The transition dipole strengths of the two sites are the same.

dx.doi.org/10.1021/jp112406h |J. Phys. Chem. B 2011, 115, 6227–6233

not depend on the method of preparing electronic excitation, i.e., whether by laser pulse or natural sunlight photon, in contrast to the concern raised by ref 28. We note that the coherence is an intrinsic property of the system's Hamiltonian.

Figure 3 gives trajectories of excitation dynamics in two-site systems (A) and linear absorption lineshapes of the ensembles (B) calculated from eqs 10−14 for a demonstration of the relation between excitation dynamics in individual PPCs and experimental observables. For the calculations, two two-site systems (a) and (b) are employed, as described in the figure caption. The lineshapes are calculated with[51−54]

$$A[\omega] = \mathrm{Re}\int_0^\infty \mathrm{d}t e^{i\omega t}\langle \sum_{m=1}^{2} \langle m|\psi(t)\rangle\langle\psi(t)|0\rangle\rangle_{\mathrm{ensemble}} \quad (15)$$

for the initial condition $\langle m|\psi(0)\rangle\langle\psi(0)|0\rangle = 1$ ($m = 1, 2$). The transition dipole strengths of the two sites are assumed to be the same. When excitation dynamics in individual PPCs shows strong wave-like motion, and the calculated absorption line shape presents the shifted peak positions and amplitudes predicted by diagonalization of the excitation Hamiltonian comprised of the Franck−Condon energies, although eq 15 does not involve such diagonalization. We note that the initial condition $\langle m|\psi(0)\rangle\langle\psi(0)|0\rangle = 1$ corresponds to the photoexcitation of the mth pigment, not that of a diagonalized state. This implies that the experimentally detected static delocalized states (generally called excitons) in the ensemble averaged behavior indicate the existence of wave-like excitation dynamics in individual PPCs. In general, optical spectroscopy provides us with the information projected onto energy eigenstates of pigments. However, this does not necessarily mean individual PPCs are always in their electronic energy eigenstates.

CONCLUDING REMARKS

We have examined a possible interpretation of the long-lived electronic quantum coherence observed in photosynthetic EET with the use of two-dimensional electronic spectroscopy. The present results demonstrate it remains possible that excitation dynamics in individual PPCs are substantially different from our intuition obtained from the RDM approach. Even in the case that the RDM does not exhibit any quantum coherent beat, dynamics of electronic excitations in individual PPCs may show wave-like motion robust against the environment-induced fluctuations. However, our purpose is not, of course, to deny that decoherence occurs. What we would like to emphasize here is that ensemble dephasing is dominant in the decay of quantum coherent oscillations observed in two-dimensional spectra and calculated with the RDM approach based on eq 1. In order to fully elucidate possible roles of quantum coherence in photosynthetic light harvesting, it is important to overcome the intrinsic coarse-grained nature of the previously observed electronic quantum coherence due to the presence of an ensemble dephasing effect. For this purpose, it is intriguing to explore dynamics of electronic excitation wavepackets in a single photosynthetic PPC or a dilute ensemble far from the thermodynamic limit. It is becoming possible to merge ultrafast spectroscopy and single-molecule detection.[55−57] Recently, Brinks et al.[57] reported the observation of vibrational wavepackets in individual molecules at ambient temperature by means of the phase-locked spontaneous light emission technique.[58,59] In such experiments a time average is made to obtain the time resolution, but as ref 57 shows, single molecules are not necessarily ergodic on the time scale of the measurement. Applications of this technique to the detection of electronic coherence in PPCs would provide further insights into photosynthetic EET and are currently in progress in our laboratory.

AUTHOR INFORMATION

Corresponding Author
*E-mail: GRFleming@lbl.gov.

ACKNOWLEDGMENT

We acknowledge an allocation of supercomputing time from the National Energy Research Scientific Computing Center. This work was supported by the Director, Office of Science, Office of Basic Energy Sciences of the U.S. Department of Energy under Contract DE-AC02-05CH11231 and the Division of Chemical Sciences, Geosciences, and Biosciences, Office of Basic Energy Sciences of the U.S. Department of Energy through Grant DE-AC03-76SF000098.

REFERENCES

(1) Cho, M. *Two-Dimensional Optical Spectroscopy*; CRC Press: Boca Raton, FL, 2009.
(2) Engel, G. S.; Calhoun, T. R.; Read, E. L.; Ahn, T.-K.; Mančal, T.; Cheng, Y.-C.; Blankenship, R. E.; Fleming, G. R. *Nature* **2007**, *446*, 782–786.
(3) Lee, H.; Cheng, Y.-C.; Fleming, G. R. *Science* **2007**, *316*, 1462–1465.
(4) Calhoun, T. R.; Ginsberg, N. S.; Schlau-Cohen, G. S.; Cheng, Y.-C.; Ballottari, M.; Bassi, R.; Fleming, G. R. *J. Phys. Chem. B* **2009**, *113*, 16291–16295.
(5) Collini, E.; Wong, C. Y.; Wilk, K. E.; Curmi, P. M. G.; Brumer, P.; Scholes, G. D. *Nature* **2010**, *463*, 644–648.
(6) Panitchayangkoon, G.; Hayes, D.; Fransted, K. A.; Caram, J. R.; Harel, E.; Wen, J.; Blankenship, R. E.; Engel, G. S. *Proc. Natl. Acad. Sci. U. S.A.* **2010**, *107*, 12766–12770.
(7) Ishizaki, A.; Fleming, G. R. *Proc. Natl. Acad. Sci. U.S.A.* **2009**, *106*, 17255–17260.
(8) van Amerongen, H.; Valkunas, L.; van Grondelle, R. *Photosynthetic Excitons*; World Scientific: Singapore, 2000.
(9) Mukamel, S. *Principles of Nonlinear Optical Spectroscopy*; Oxford University Press: New York, 1995.
(10) Nielsen, M. A.; Chuang, I. L. *Quantum Computation and Quantum Information*; Cambridge University Press: New York, 2000.
(11) Schlosshauer, M. A. *Decoherence and the Quantum-to-Classical Transition*; Springer: Berlin, 2007.
(12) Zurek, W. H. *Phys. Today* **1991**, *44*, 36–44.
(13) Zurek, W. H. *Prog. Theor. Phys.* **1992**, *89*, 281–312.
(14) Joos, E.; Zeh, H. D.; Kiefer, C.; Giulini, D. J. W.; Kupsch, J.; Stamatescu, I.-O. *Decoherence and the Appearance of a Classical World in Quantum Theory*, 2nd ed.; Springer: Berlin, 2003.
(15) Ehrenfest, P. *Z. Phys.* **1927**, *45*, 455–457.
(16) Mott, N. F. *Proc. Cambridge Philos. Soc.* **1931**, *27*, 553–560.
(17) Billing, G. D. *The Quantum Classical Theory*; Oxford University Press: New York, 2003.
(18) Kapral, R. *Annu. Rev. Phys. Chem.* **2006**, *57*, 129–157.
(19) Jang, S.; Cheng, Y.-C.; Reichman, D. R.; Eaves, J. D. *J. Chem. Phys.* **2008**, *129*, 101104.
(20) Mohseni, M.; Rebentrost, P.; Lloyd, S.; Aspuru-Guzik, A. *J. Chem. Phys.* **2008**, *129*, 174106.
(21) Palmieri, B.; Abramavicius, D.; Mukamel, S. *J. Chem. Phys.* **2009**, *130*, 204512.
(22) Ishizaki, A.; Fleming, G. R. *J. Chem. Phys.* **2009**, *130*, 234111.
(23) Thorwart, M.; Eckel, J.; Reina, J. H.; Nalbach, P.; Weiss, S. *Chem. Phys. Lett.* **2009**, *478*, 234–237.

(24) Womick, J. M.; Moran, A. M. *J. Phys. Chem. B* **2009**, *113*, 15747–15759.
(25) Scholes, G. D. *J. Phys. Chem. Lett.* **2010**, *1*, 2–8.
(26) Tao, G.; Miller, W. H. *J. Phys. Chem. Lett.* **2010**, *1*, 891–894.
(27) Sarovar, M.; Ishizaki, A.; Fleming, G. R.; Whaley, K. B. *Nat. Phys.* **2010**, *6*, 462–467.
(28) Mančal, T.; Valkunas, L. *New J. Phys.* **2010**, *12*, 065044.
(29) Huo, P.; Coker, D. F. *J. Chem. Phys.* **2010**, *133*, 184108.
(30) Olaya-Castro, A.; Lee, C. F.; Olsen, F. F.; Johnson, N. F. *Phys. Rev. B* **2008**, *78*, 085115.
(31) Plenio, M. B.; Huelga, S. F. *New J. Phys.* **2008**, *10*, 113019.
(32) Rebentrost, P.; Mohseni, M.; Kassal, I.; Lloyd, S.; Aspuru-Guzik, A. *New J. Phys.* **2009**, *11*, 033003.
(33) Caruso, F.; Chin, A. W.; Datta, A.; Huelga, S. F.; Plenio, M. B. *J. Chem. Phys.* **2009**, *131*, 105106.
(34) Cao, J.; Silbey, R. J. *J. Phys. Chem. A* **2009**, *113*, 13825–13838.
(35) Wu, J.; Liu, F.; Shen, Y.; Cao, J.; Silbey, R. J. *New J. Phys.* **2010**, *12*, 105012.
(36) Hoyer, S.; Sarovar, M.; Whaley, K. B. *New J. Phys.* **2010**, *12*, 065041.
(37) Sarovar, M.; Cheng, Y.-C.; Whaley, K. B. *Phys. Rev. E* **2011**, *83*, 011906.
(38) Scholak, T.; de Melo, F.; Wellens, T.; Mintert, F.; Buchleitner, A. *Phys. Rev. E* **2011**, *83*, 021912.
(39) Haken, H.; Strobl, G. *Z. Phys.* **1973**, *262*, 135–148.
(40) Leegwater, J. A. *J. Phys. Chem.* **1996**, *100*, 14403–14409.
(41) Gaab, K. M.; Bardeen, C. J. *J. Chem. Phys.* **2004**, *121*, 7813–7820.
(42) Renger, T.; May, V.; Kühn, O. *Phys. Rep.* **2001**, *343*, 137–254.
(43) Ishizaki, A.; Calhoun, T. R.; Schlau-Cohen, G. S.; Fleming, G. R. *Phys. Chem. Chem. Phys.* **2010**, *12*, 7319–7337.
(44) May, V.; Kühn, O. *Charge and Energy Transfer Dynamics in Molecular Systems*; Wiley VCH: Weinheim, Germany, 2004.
(45) Kubo, R.; Toda, M.; Hashitsume, N. *Statistical Physics II: Nonequilibrium Statistical Mechanics*, 2nd ed.; Springer-Verlag: New York, 1995.
(46) Tully, J. C.; Preston, R. K. *J. Chem. Phys.* **1971**, *55*, 562–572.
(47) Zwanzig, R. *J. Stat. Phys.* **1973**, *9*, 215–220.
(48) Kubo, R. *Adv. Chem. Phys.* **1969**, *15*, 101–127.
(49) Hamm, P.; Lim, M.; Hochstrasser, R. M. *Phys. Rev. Lett.* **1998**, *81*, 5326–5329.
(50) Wang, H.; Song, X.; Chandler, D.; Miller, W. H. *J. Chem. Phys.* **1999**, *110*, 4828–4840.
(51) Heller, E. J. *J. Chem. Phys.* **1978**, *68*, 2066–2075.
(52) Heller, E. J. *J. Chem. Phys.* **1978**, *68*, 3891–3896.
(53) Myers, A. B. *J. Opt. Soc. Am. B* **1990**, *7*, 1665–1672.
(54) Myers, A. B.; Markel, F. *Chem. Phys.* **1990**, *149*, 21–36.
(55) van Dijk, E. M. H. P.; Hernando, J.; García-López, J.-J.; Crego-Calama, M.; Reinhoudt, D. N.; Kuipers, L.; García-Parajó, M. F.; van Hulst, N. F. *Phys. Rev. Lett.* **2005**, *94*, 078302.
(56) Gerhardt, I.; Wrigge, G.; Zumofen, G.; Hwang, J.; Renn, A.; Sandoghdar, V. *Phys. Rev. A* **2009**, *79*, 011402.
(57) Brinks, D.; Stefani, F. D.; Kulzer, F.; Hildner, R.; Taminiau, T. H.; Avlasevich, Y.; Mullen, K.; van Hulst, N. F. *Nature* **2010**, *465*, 905–908.
(58) Scherer, N. F.; Carlson, R. J.; Matro, A.; Du, M.; Ruggiero, A. J.; Romero-Rochin, V.; Cina, J. A.; Fleming, G. R.; Rice, S. A. *J. Chem. Phys.* **1991**, *95*, 1487–1511.
(59) Scherer, N. F.; Matro, A.; Ziegler, L. D.; Du, M.; Carlson, R. J.; Cina, J. A.; Fleming, G. R. *J. Chem. Phys.* **1992**, *96*, 4180–4194.